Signatures of internal feedback and trajectory control during goal-directed finger and whole-arm reaching movements

Niranjan Chakrabhavi [a,b,*], Varadhan SKM [b], Ashitava Ghosal [c], Aditya Murthy [a,*]

[a]Centre for Neuroscience, Indian Institute of Science, Bengaluru 560012, India. [b]Department of Applied Mechanics and Biomedical Engineering, Indian Institute of Technology Madras, Chennai 600036, India. [c]Department of Mechanical Engineering, Indian Institute of Science, Bengaluru 560012, India.

[*]Corresponding Authors – Niranjan Chakrabhavi (niranjanc@iisc.ac.in) and Aditya Murthy (adi@isc.ac.in).

Abbreviated title: Internal feedback enables rapid trajectory control.

Keywords: motor control, trajectory planning, variability, and correlation.

Number of Pages: 41 (including figures)

This pdf file includes:

1. Figures 1 to 9
2. Tables 1 to 3

Number of words:

1. Abstract - 238
2. Significance Statement - 90
3. Introduction – 552
4. Discussion – 1418

Author Contribution: NC conceived the study; NC and VSKM designed the finger experiment; NC and AM designed the arm experiment; NC collected data and performed the data analysis; AM and AG supervised the analysis; NC and AM wrote the manuscript; AG and VSKM reviewed the manuscript.

Conflict of Interest Statement: The authors declare no conflict of interest.

Abstract

Goal-directed behaviors involve the execution of a variety of eye, hand, and finger movements that follow invariant kinematics consisting of straight-line trajectories and bell-shaped velocity profiles. Despite the presence of neuromotor noise and distinct biomechanics such motions are performed with ease and reasonable accuracy. A fundamental unresolved issue in the field is to determine and delineate the extent to which these trajectories are planned or whether they are a consequence of trajectory-free online control. In this study, we address this question using Spearman's rank correlation, zero-crossing rate and *z*-scores and analyze within-trial variability to investigate differences in the time evolution of trajectories during the presence or absence of a goal in finger and whole-arm reaching movements. We found that the central nervous system (CNS) implements control to follow an average trajectory, where goal-directed movements show an enhanced degree of trajectory control. Further, by performing the analysis on the actual timing, we found behavioral signatures of rapid control that might operate on these planned trajectories as early as 30 ms in finger movements and 16.67 ms in whole-arm reaching movements which are too early for trajectory control to be derived from delayed sensory feedback. The analysis also revealed that the controller gains varied along the movement and peaked distinctly at an early (20 %) and a late (90 %) phases of movement, suggesting that trajectory control may be accomplished through virtual way-point objectives during the execution of the movement.

Significance Statement

The extent to which reaching movements reflect the unfolding of a prespecified trajectory plan or whether they arise from a trajectory-free online control has remained a vexing issue for motor theorists. Using novel measures of control during the movement such as Spearman's rank correlation, zero-crossing rate and trends in *z*-scores, we investigated goal-directed finger and whole-arm reaching movements and demonstrated that the CNS implements rapid control to follow a planned trajectory, especially during early and late phases of movement. Our results provide novel constraints for computational theories of motor control.

Introduction

Normative goal-directed movements are characterized by invariant-kinematic patterns that consist of straight-line trajectories with bell-shaped velocity profiles that scale with movement amplitude and speed (Morasso, 1981). Numerous psychophysical and neurophysiological studies highlight the notion that movement attributes are represented/programmed in the central nervous system well before execution (Keele, 1968; Rosenbaum, 1985; Dick et al., 1986; Morris et al., 1994; Moran and Schwartz, 1999; Padoa-Schioppa et al., 2002; Churchland et al., 2006; Summers and Anson, 2009). Such results have motivated the use of internal models wherein a complete specification of a trajectory can be made, in principle, before its implementation (Bizzi et al., 1984; Wolpert et al., 1995; Wolpert and Kawato, 1998; Desmurget and Grafton, 2000; Wolpert and Ghahramani, 2000). However, other influential models of motor control suggest that only certain critical features of the movement such as the endpoint or desired displacement need to be specified in advance (Todorov and Jordan, 2002; Desmurget and Grafton, 2003; Scott, 2004); here, the neural representation specifying movement trajectories may only be generated dynamically in real-time during movement execution as a consequence of sensory feedback that is sensitive to the demands of the task. Thus, it remains unclear whether movement attributes such as trajectories are planned before movement execution or whether they are derived from online feedback control.

One feature that in principle can distinguish between planned and derived movement trajectories is the timing of their respective control signals that are necessary to mitigate the effects of motor noise that is a ubiquitous property of muscle and neural activity. In the context of planned movement trajectories, a comparison between desired and current states can be used as an error signal to control movements in the absence of actual sensory information

(Gordon and Ghez, 1987; Kawato et al., 2003; Richardson et al., 2011). In contrast, sensory feedback control relies on relatively delayed sensory (> 50 ms) feedback to make meaningful corrections during the movement (Todorov and Jordan, 2002; Wolpert et al., 2011). While such rapid control has been studied in the context of fast saccadic eye movements (Kawato, 1999; Gaveau et al., 2003; Richardson et al., 2011) as well as rapid corrections to task-related errors using predictive error-related negativity (ERN) (LoTemplio et al., 2023), distinct signatures of such rapid control prior to sensory feedback in the context of normative movements have not been experimentally demonstrated to the best of our knowledge.

Using the distinction between the temporal properties of these two forms of control, we used a novel approach to compare the trajectory profiles in reaching movements which were either goal/task driven versus a similar movement in the absence of a goal/task to determine whether trajectory control is based exclusively on sensory feedback (Liu and Todorov, 2007; Pruszynski et al., 2011) or whether it can also involve internal feedback control as predicted by some computational theories of motor control (Harris and Wolpert, 1998; Desmurget and Grafton, 2000). With the use of Spearman's rank correlation, the zero-crossing rate, and by tracking how *z*-scores changed over the time course of movement, we show that the motor system can plan a kinematic trajectory which can be guided by internal feedback control. Further, by examining the temporal changes in correlation and the zero-crossing rate, we showed that trajectory control is most prominent during the initial and final phases of the movement.

Materials and Methods

Experiment 1 – Individual cyclic flexion-extension movement of fingers

A detailed description of the experiment can be found in our previously published article (Chakrabhavi and Skm, 2019). In brief, participants sat on a height-adjustable chair and

positioned their right dominant arm at ~30^0 shoulder flexion and ~120^0 elbow extension as they rested their forearm and palm on a flat surface in neutral (pronation-supination) forearm posture (Fig. 1A). The forearm and the thumb were constrained by a strap while the other four fingers of interest were suspended in air and free to move. The movements of phalanges of all four fingers were recorded using electromagnetic tracking sensors (Micro Sensor 1.8^{TM}, Liberty tracking system, Polhemus Inc., Colchester, VT, USA). The task was designed on LabVIEW (National Instruments Corp, Austin, TX, USA) and the data was sampled at a frequency of 100 Hz. A total of eight healthy right-handed subjects (5 males) participated in this study. The experiment was approved by the institute ethics committee at IIT Madras, and all the participants provided a written informed consent before the start of the experiment.

On any given attempt, subjects were required to maintain a predefined wrist posture (0^0 neutral, 30^0 flexion or 30^0 extension) and asked to make cyclic flexion-extension movements (0.75 Hz movement frequency) at the metacarpophalangeal joint with one of the instructed fingers (among index, middle, ring, and little) between 75 ± 10 % of its maximum flexion-extension limits and to ignore any movements in the non-instructed fingers. The effect of finger enslavement led to involuntary movements in the non-instructed fingers (Li et al., 2004). For this analysis, we considered movements performed by instructed finger as goal-directed and the movements in non-instructed finger as non-goal condition. Each attempt lasted for 32 seconds with an initial 2 seconds of rest followed by 30 seconds of cyclic flexion-extension movements (Fig. 1B). Real-time visual feedback of the distal phalange of the instructed finger was provided on the screen, along with its movement landmarks, and an audio metronome was played at 1.5 Hz to ensure the amplitude and timing of the instructed finger movement, respectively. There were 36 attempts (3 wrist postures x 4 instructed fingers x 3 attempts each) in total. Data from the distal phalanges of each of the four fingers at neutral wrist posture (0^0) were used in this study. Specifically, each attempt was segmented into several half-cycles

comprising of movements from flexion (local peaks of middle finger trace in Fig. 1B) to subsequent extension (local troughs of middle finger trace in Fig. 1B) of instructed finger and the same time stamps were used to segment the movements of non-instructed fingers. The half cycles were then resampled to 100 equal spaced segments to analyze control with respect to a normalized percentage time scale as in Figs. 3 and 4, whereas the first 300 ms were used for the analysis on an actual time scale in Fig. 3C.

Experiment 2,3 – Discrete horizontal reaching movements by dominant and non-dominant arms and fast and slow movements

Participants: Twenty-five healthy right-handed subjects (15 subjects for experiment 2, and 10 subjects for experiment 3; 21 males; Age [min-max]: 21-32) participated in the study. The experiment was approved by the institute ethics committee at IISc Bengaluru, and all the participants provided a written informed consent before the start of the experiment. The Edinburgh Handedness Inventory (Oldfield, 1971) was used to evaluate their dominant arm.

Experimental Setup: Subjects sat on a chair with a backrest to minimize the movements of the clavicle (collar bone) and their dominant or the non-dominant arm was required to rest on a smooth elevated table to facilitate horizontal reaching movements (Fig. 1C). They were mounted with five electromagnetic 3D motion tracking sensors (Teardrop Mini sensors, 240Hz, Liberty tracking system, Polhemus Inc., Colchester, USA) on the surface of the skin at the sternoclavicular joint (neck), right or left acromion process (right or left shoulder) depending on the task of interest, lateral epicondyle (lateral aspects of the elbow), dorsal tubercle of radius (wrist) and the dorsal aspect of the hand respectively, by a 3M micropore surgical tape. The sensor on the dorsal side hand was used for the current analysis. The lights were switched off in the experimental room to occlude the subject's vision of their arm posture during the movement. Subjects were required to hold an endpoint robotic manipulandum

156 (KINARM, 240 Hz, BKIN Technologies Ltd., Kingston, Canada) and perform a center out
157 discrete horizontal planar reaching movement as required by the task. During the reaching
158 movement, the subjects were required to look at the stimulus screen (LCD Screen, 60 Hz) in
159 front of them where a circular shaped cursor on the screen was mapped onto the position of the
160 held manipulandum. All the experimental protocols were coded and executed on
161 TEMPO/VideoSYNC Software (Reflective Computing, St. Louis, MO, USA). The dataset was
162 post-processed using MATLAB interface (MathWorks, Massachusetts, USA).

163 Task Structure: A white fixation box (hollow square, 2 cm) appeared at the center of
164 the workspace where the subjects were required to position the pink-colored cursor inside it by
165 moving the manipulandum with one of their arms (Fig. 1D). Once they fixated at the center for
166 500 ms, a red-colored target (filled square, 1 cm) appeared on the screen at an eccentricity of
167 12 cm from the center at any of the 8 directions (0^0, 45^0, 90^0, 135^0, 180^0, 225^0, 270^0, or 315^0).
168 Subjects made smooth unperturbed goal directed movement towards the target location as soon
169 as the central fixation box disappeared, which was after a hold time of 1000 ms. After initiating
170 the movement, they were given 1000 ms to reach the target location. Once they reached the
171 target, they were required to stay there for 500 ms to successfully complete one trial. The
172 successful completion of the trial was indicated to the subjects by providing an auditory tone.
173 The inter-trial interval was set to 1500 ms where the cursor had to be brought back to the central
174 fixation box for the initiation of subsequent trial. These were called return movements and were
175 not associated with reward. Sample movement traces of goal and return movements by
176 dominant arm and the goal directed movements by the non-dominant arms are shown in Fig.
177 1E. If the subject did not fixate enough at the center or at the target, or if they were not able to
178 execute movements within the required time, the trial was aborted. The experiment was
179 conducted such that ~40 successful trials were recorded in each of the 8 directions (5 out of 15
180 subjects performed ~60 trials towards 0^0 and 45^0, and ~20 trials towards other directions). The

same task was now repeated with the other arm and the sequence of recruitment of the arms were randomized across subjects.

Experiment-3 on fast and slow movements was designed similarly with some minor modifications. The target color was used to cue the subjects about the speed of movement – green for fast (reach within 400 ms) and red (reach from 600-1000 ms) for slow movements and that the trials were randomly interleaved. For this experiment, the subjects used their dominant right arm and performed movements towards 0^0 and 45^0 directions only.

Data pre-processing: The motion data from the 3D motion tracking sensors on the hand was low-pass filtered with a cut-off frequency of 20 Hz using a fourth order zero lag Butterworth filter (Scholz et al., 2000). The time at which the hand crossed 5 % of its maximum speed during the acceleration and deceleration phases respectively were noted (Georgopoulos et al., 1982; Scott et al., 2001; Chakrabhavi and Skm, 2019). The time of onset and the end of movement were identified by descending along the velocity curve from the 5 % mark to whenever it reached zero for the first time. The motion data was then resampled to 100 equally spaced segments to normalize for time (percentage time) across various trials in analysis of Figs. 5-9, while the data for the first 500 ms during the movement was used for the analysis of actual time scale in Fig. 5C and 7D. For Figs. 5A, 5C and 6A, fixation condition was defined as the time between movement onset (t = 0) to 1000 ms prior to the onset, in the negative direction of time, when the cursor was inside the fixation box. We used this as a reference to compare goal directed movements that were performed subsequently.

Data analysis

The displacement data (in the direction of flexion- extension) of the four fingers (index, middle, ring, and little) from Experiment 1 (Chakrabhavi and Skm, 2019), the displacement in X and Y directions (horizontal movement) of the hand from Experiment 2 and Experiment 3

were used for the analysis. The number of trials in each of the fingers were selected such that the initial postural variability was equated between the goal and the corresponding non-goal fingers. For the goal and return movements by the arm, the initial variability in hand postures were equated along both X and Y co-ordinates of each of the directions of movement. For dominant and non-dominant arm movements, the equalization of initial variability was performed by considering the similarity of movements with respect to both arms. For example, the initial variability along 0^0 directed movements by the dominant arm were equated with the 180^0 directed movements performed by the non-dominant arm. The initial variability was similar for fast and slow movements as the trials were randomly interleaved and the trials starting within 2 standard deviations around the mean were selected for the analysis in this case. The equalization of initial variability was done to eliminate the influence of initial variance on the correlation analysis and restricted to report differences in correlation caused due to differences in movement execution.

For any given task, and at every normalized time point, each trial was assigned a *z*-score using Eq. (1), by subtracting its amplitude from the mean and divided it by the inter-trial standard deviation (Fig. 2). Subtraction from the mean was performed to track how the trajectories across different trials moved relative to the average trajectory, and that they were normalized by the standard deviation, as it changed through the course of movement (Figs. 7A and 8A). A sample of movement trajectories (grey) of the arm, directed towards 0^0, is shown in Fig. 2C and the *z*-scores of the corresponding red and blue trajectories are shown in Fig. 2D. The motivation of this procedure was to analyze the within trial variability by observing changes in the *z*-scores of each trial along the duration of movement by providing a unitless approach to study such variability.

$$z_{i,j} = \frac{A_{i,j} - \mu_j}{\sigma_j} \qquad (1)$$

where $z_{i,j}$ is the z-score of trial – i at time – j of the trajectory with amplitude $A_{i,j}$. Parameters μ_j and σ_j are the inter-trial average and inter-trial standard deviation of amplitude (A) across n trials at time j. $A_{n\,x\,T}$ is the matrix representing amplitude of trajectories with n trials and T = 101, normalized time instances.

To investigate the structure of within trial variability we performed Spearman's rank correlation (Hollander et al., 2013) between the z-scores at the start of movement $z(0)$, with the z-scores at subsequent time instances $z(j)$. In Fig. 2, we have depicted two distinct cases of online control. On the left side (Fig. 2A), the representative trajectories crossover each other such that their relative ranks change during the movement. For example, the rank order of trajectories - red, green, blue, and pink (top to bottom) at time t = 0, changes to green, pink, red, and blue at time $t = j$. This leads to decorrelation among their ranks and a decrease in Spearman's correlation coefficient (ρ), because of implementation of active online control. Conversely, on the right side (Fig. 2B), the order of trajectories remains the same throughout the movement and that the trajectories never converge towards their average trajectory, thereby resulting in high ρ (close to 1) and weaker/lack of implementation of online control. We perform the correlation analysis from movement onset to the end of movement (t = 0 to 100 %), to obtain a time varying trajectory of correlation coefficient, $\rho(t)$. We chose the Spearman's correlation coefficient as we were particularly interested in the crossovers among trajectories, independent of changes in inter-trial standard deviation (Figs. 7A and 8A) during the course of the movement. We investigated the average decorrelation ($\bar{\rho}$) over the entire movement duration to quantify the extent of control. We then fit a logistic function $\rho fit(t)$, over $\rho(t)$ for each of the subjects and used parameter β to quantify the rate of decrease of $\rho(t)$ using Eq. (2).

$$\rho fit(t) = a + \frac{1}{1 + e^{\beta(\rho(t) - \mathrm{c})}} \qquad (2)$$

To substantiate our hypothesis, we computed a dispersion measure for the time normalized trajectories ($A_{n \times T}$) by taking the ratio of average inter-trial standard deviation over the time course, with the average range of movement during the *n* trials, in Eq. (3). We divided variability with the range, to account for differences in movement amplitude in the finger experiment. We then correlated the average decorrelation ($\bar{\rho}$) with its average dispersion measure (or with standard deviation in Fig. 7C and 8C) expecting that a reduction in $\bar{\rho}$ leads to lower dispersion.

$$Dispersion = \frac{\frac{1}{T}\sum_{j=1}^{T}\sqrt{\frac{\sum_{i=1}^{n}\left(A_{i,j}-\mu_j\right)^2}{n-1}}}{\frac{1}{n}\sum_{i=1}^{n}|\max(A_i)-\min(A_i)|} \qquad (3)$$

where μ_j is the average of amplitude (A) across *n* trials at time *j* and A_i is the trajectory on trial – *i*.

For Fig. 3D and 5D, the correlation analysis was performed using a similar technique described earlier but between consecutive 10 % - time instances. At any percentage time point, the value of Spearman's correlation (ρ_c) was computed between the *z*-scores of trajectories at that time point with respect to an earlier 10 % - time instance. For example, at t = 20 %, the correlation analysis was performed between postures at 20 % with that of the postures at 10 % movement duration. This analysis was restricted to goal directed movements.

We further investigated whether the implemented online control was intended to follow an average planned trajectory. In Fig. 2D, the z = 0, represents an average trajectory (dashed line), and the red trajectory crosses the dashed line three times showing a strong trajectory control while the blue does not cross the dashed line at all showing weaker trajectory control. To quantify this effect, we computed a zero-crossing rate (*ZCR*) from the *z*-scores of movement trajectories, which was defined as per Eq. (4). A larger *ZCR* imply a greater trajectory control. A zero-crossover was considered valid only if the amplitude of transition (Δz) at the time of

cross-over was greater than 0.01. The threshold was chosen as the *ZCR* under this value did not yield significant differences between goal and non-goal conditions and can be attributed to noise. For arm movements, the *ZCR* plotted in Figs. 6-8, was further averaged across *X* and *Y* co-ordinates and along all the movement directions. We also computed *ZCR* during early (0 to 33 %), middle (34 to 66 %) and late (67 to 100 %) phases of movements in Figs. 4C and 6C.

$$ZCR = \frac{Total\ number\ of\ valid\ zero\ crossings}{Total\ number\ of\ trials} \qquad (4)$$

To support evidence of trajectory control, the starting postures of goal movements in fingers (Fig. 4B) and arm (Fig. 6B), were divided into two groups, the ones which were farther away ($|z| > 0.5$, purple in Fig. 4B and red in Fig. 6B) and the ones closer ($|z| <= 0.5$, black) to the average initial posture ($z = 0$). The average *z*-scores (across trials) were tracked along the time course of movement to check the propensity of these two groups to converge towards an average planned trajectory ($z = 0$, between 0 – 100 % movement phases). If the central nervous system intended to follow an average trajectory, the group which was farther away from the initial posture should show greater convergence towards the average trajectory than the closer ones. The difference in *z*-scores at 0th (initial) and 20th percentile time points were used to quantify this effect.

Statistics

The data were checked for normality using the Kolmogorov-Smirnov test. We performed pairwise *t*-test for paired comparisons and two-sample *t*-test for independent comparisons if the data were normal, and Wilcoxon signed rank test and Wilcoxon rank-sum test for paired and independent comparisons otherwise. For more than two sample paired

comparisons, we performed repeated measures ANOVA. Multiple pairwise comparisons were reported with Bonferroni corrections.

Result

Online control of goal and non-goal finger movements

The differences in the magnitude of online control among goal and non-goal fingers were quantified by computing the average decorrelation ($\bar{\rho}$) during the movement (Fig. 3A). A two-way repeated measures ANOVA (4 finger-tasks x 2 finger-type, goal or non-goal) showed that the $\bar{\rho}$ of goal finger was significantly different from the non-goal finger ($P < 0.001$). By comparing goal and the corresponding non-goal fingers in a pairwise method it was observed that the extent of decorrelation was highest in the goal fingers (Table 1).

The dynamics of online control in goal and non-goal fingers were teased apart by computing the rate of decrease (β) in correlation co-efficient, $\rho(t)$ (Fig. 3A). A logistic function was fitted to the dataset to find β (median explained variance = 0.95). A two-way repeated measures ANOVA (4 finger-tasks x 2 finger-types, goal or non-goal) showed that the rate of decrease of $\rho(t)$ was significantly different across goal and non-goal fingers ($P < 0.001$). Broadly, by performing pairwise comparisons, it was found that the rate of decrease of $\rho(t)$ in the goal directed finger was significantly higher than the non-goal non-neighboring fingers but was from different from that of neighboring fingers (Table 2).

Further, we checked if the average decorrelation in finger trajectories was systematically associated with the average trajectory dispersion (Fig. 3B) and found that they were tightly correlated (Spearman's $\rho = 0.9$, $P < 0.001$), and the average dispersion of goal finger (median = 0.073) was significantly less than that of non-goal neighboring (median = 0.143, $P < 0.001$) and non-neighboring (median = 0.573, $P < 0.001$) fingers. Thus, a higher

323 degree of trajectory decorrelation was associated with lesser dispersion in trajectories and vice
324 versa. As goal fingers were associated with varying movement amplitudes, we compared $\rho(t)$
325 of all four goal fingers to check the sensitivity of the correlation analysis to the differences in
326 the range of movement among them. A one-way repeated measures ANOVA on the goal
327 fingers revealed that the $\bar{\rho}$ were not significantly different (P = 0.72) and the rate of decrease
328 of $\rho(t)$ were also not significantly different across goal fingers (P = 0.52) but the range of
329 movement were significantly different between them (P < 0.001), with index (mean ± SEM:
330 10.63 ± 0.27 cm) and little (mean ± SEM: 7.42 ± 0.27 cm) fingers having the highest and
331 lowest movement ranges, respectively.

332 Next, we quantified the differences in the time of control by performing the correlation
333 analysis on the actual timing, from movement onset to 300 ms into the movement. We found
334 that ρ(t) of the goal finger (dark purple) diverged significantly from that of non-goal
335 neighboring (medium purple) and non-neighboring (light purple) fingers at 50 ms and 30 ms,
336 respectively (Fig. 3C).

337 Motivated by the previous findings, we examined whether trajectory control was
338 constant or occurred during distinct phases along the movement duration. For this, we
339 performed the correlation analysis on the goal finger movements on consecutive 10 % - time
340 instances and found that the controller acted discretely with two prominent troughs in $\rho_c(t)$ at
341 20th (binominal P < 0.001) and 90th percentile time (binominal P < 0.001) points (Fig. 3D)
342 suggesting the presence of early and late phases of control.

343

344 **Trajectory control of goal-directed finger movements**

345 We tested the zero-crossing rate (*ZCR*) of goal and non-goal fingers during the four
346 different instructed finger tasks to probe the propensity of trajectories to follow an average
347 trajectory (Fig. 4A and Fig. 2D for the method of computation). A two-way repeated measures

348 ANOVA (4 finger-tasks x 2 finger-type, goal or non-goal) revealed that the *ZCR* of goal finger
349 was significantly different from that of non-goal fingers ($P < 0.001$). By performing pairwise
350 comparison between goal and non-goal fingers it was found that the goal finger had the highest
351 *ZCR* in all the four tasks (Table 3). To support this further, we divided initial postures of goal
352 fingers into two groups (Fig. 4B), the ones farther away ($|z| > 0.5$, purple) and the ones closer
353 ($|z| <= 0.5$, black) to the average initial posture ($z = 0$) and found that the away group had a
354 significantly greater propensity to converge towards an average trajectory (mean ± SEM: 0.43
355 ± 0.02) than the closer ones (0.09 ± 0.02, $P < 0.001$). Also, the farther away group had a
356 significantly greater covergence in the goal finger as compared to that in non-goal fingers (0.02
357 ± 0.01, $P < 0.001$).

358 To substantiate the evidence of a temporal structure of control in Fig. 3D, we computed
359 the *ZCR* of goal finger movements across three movement segments (Fig. 4C); early (0 to 33
360 %, light grey), middle (34 to 66 %, medium grey), and late (67 to 100 %, dark grey) phases of
361 movement duration and found that the *ZCR* was significantly higher during early (mean ±
362 SEM: 0.42 ± 0.01) and late (0.47 ± 0.01) phases as compared to the middle phase (0.25 ± 0.02;
363 Adj. $P < 0.001$ for both the comparisons).

364

365 **Online control of goal directed whole-arm movements**

366 We investigated whether the correlation analysis performed on finger movements could
367 be extended to whole-arm reaching movements and if there were systematic control signatures
368 in goal movements. We performed the correlation analysis (Fig. 5A) and found that the $\bar{\rho}$ in
369 goal movements (mean ± SEM: 0.38 ± 0.02) was significantly less than that during fixation
370 (0.98 ± 0.003, $P < 0.001$). A logistic function was fit over $\rho(t)$ (median explained variance =
371 0.94) to find the rate of decrease (β) in correlation and it was found to be significantly higher
372 in goal movements (mean ± SEM: 0.143 ± 0.005) than the fixation (0.063 ± 0.028, $P < 0.005$).

Further, the average decrease in correlation in goal movements was significantly associated with the respective trajectory dispersion (Pearson's $r = 0.57$, $P = 0.02$, Fig. 5B). To estimate the timing at which the feedback control was initiated in goal directed movements, we looked at the time at which $\rho(t)$ of goal movements significantly diverged from that of fixation and found that it occurred at 16.67 ms (Fig. 5C).

Further, to investigate whether such online control was constant or varied across different phases of movement, we performed the correlation analysis of goal directed movements on consecutive 10 % - time instances, $\rho_c(t)$. As was observed in finger movements, we found two distinct troughs at 20th (binomial $P < 0.001$) and around 90th (trough shared between 80th and 90th percentiles, binomial $P < 0.001$ for both time stamps, shared across the participants) percentile time instances, indicating early and late phase of control, respectively (Fig. 5D).

Trajectory control of goal-directed arm movements

As we did in finger movements, we computed the zero-crossing rate (*ZCR*) for goal movements and compared them during fixation and found that the *ZCR* of goal movements (mean ± SEM: 1.47 ± 0.03) was significantly greater than that during fixation (0.09 ± 0.01; $P < 0.001$, Fig. 6A). Similar to the analysis in the previous section, we divided the initial postures of goal movements into two groups (Fig. 6B), the ones farther away ($|z| > 0.5$, red) and the ones closer ($|z| <= 0.5$, black) to the average initial posture ($z = 0$) and found that the away group had a significantly greater propensity to converge towards an average trajectory (mean ± SEM: 0.57 ± 0.02) than the closer ones (0.12 ± 0.02, $P < 0.001$).

To substantiate the evidence for distinct phases of control, the *ZCR* of goal directed arm movements were computed across three movement segments (Fig. 6C); early (0 to 33 %, light red), middle (34 to 66 %, medium red), and late (67 to 100 %, dark red) phases of movement

duration and found that the *ZCR* was significantly higher during early (mean ± SEM: 0.57 ± 0.01) and late (0.52 ± 0.01) phases as compared the middle phase (0.38 ± 0.05; Adj. $P < 0.001$ for both the comparisons), similar to that of finger movements.

Differences in control between goal and return movements

As differences in control measures between fixation and reaches maybe related to differences in postural versus movement control, we tested whether these signatures of active control were also visible between similar movements but having different degree of dispersions. For this, we took advantage of movements that were made back to the fixation spot since the maximum inter-trial standard deviation of return movements (mean ± SEM: 1.46 ± 0.05 cm) was significantly greater than the goal movements (mean ± SEM: 1.17 ± 0.05 cm, $P < 0.001$, Fig. 7A). We found that $\bar{\rho}$ in goal movements (mean ± SEM: 0.38 ± 0.02) was significantly less than that of return movements (0.41 ± 0.01, $P = 0.04$, Fig. 7B). This difference in $\bar{\rho}$ was prominent in the first 50 % of the movement duration (goal: 0.5 ± 0.02, return: 0.61 ± 0.01, $P < 0.001$). A logistic function was fit over $\rho(t)$ (median explained variance = 0.97) to find the rate of decrease (β) and it was found to be significantly higher in goal movements (mean ± SEM: 0.143 ± 0.05) than the return movements (0.099 ± 0.006, $P < 0.001$). Also, the $\bar{\rho}$ in goal movements was significantly associated with their respective trajectory dispersion (Pearson's $r = 0.53$, $P = 0.002$). Interestingly, the $\bar{\rho}$ during the first 20 % - time duration was significantly less in goal movements (mean ± SEM: 0.81 ± 0.01) than the return movements (0.91 ± 0.01, $P < 0.001$) and we found that it was significantly associated with the respective maximum standard deviation (Pearson's $r = 0.464$, $P = 0.009$) which occurred much later during the movement (Fig. 7C). This association was conserved for the duration as early as 10 % into the movement execution (Pearson's $r = 0.426$, $P = 0.018$). These differences between goal and return movements were not because of movement kinematics as the maximum

423 movement speeds were not significantly different across the conditions (P = 0.62). We
424 estimated the timing of control (Fig. 7D) by observing the time at which $\rho(t)$ of goal
425 movements significantly deviated from that of return movements and found that it happened at
426 a median time of 16.67 ms across subjects (Fig. 7E). Further, the maximum change in $\rho(t)$ for
427 goal movements (mean ± SEM: 128.33 ± 5.62 ms) and was significantly earlier than for non-
428 goal movements (201.38 ± 8.02 ms, $P < 0.001$).

429 We also computed *ZCR* to find the propensity of the trajectories to follow an average
430 trajectory and found that the *ZCR* of goal movements (mean ± SEM: 1.48 ± 0.03) was
431 significantly greater than the return movements (1.32 ± 0.02, $P < 0.001$, Fig. 7F). Also, the
432 farther away group in goal movements (mean ± SEM: 0.57 ± 0.02, Fig. 6B) had significantly
433 greater propensity to converge towards the average trajectory than during return movements
434 (0.33 ± 0.02, $P < 0.001$).

435

436 **Differences in control between dominant and non-dominant arm movements**

437 As expected, the trajectories of the dominant arm (average SD, mean ± SEM: 0.63 ±
438 0.02) had significantly less inter-trial variability (Fig. 8A) than those with the non-dominant
439 arm (0.69 ± 0.02, P = 0.004). Although the movement kinematics were not significantly
440 different between dominant (maximum speed, mean ± SEM: 23.38 ± 0.98 cm/s) and non-
441 dominant arms (24.38 ± 0.72 cm/s, P = 0.33, Fig. S1D). We found that the $\bar{\rho}$ was significantly
442 lesser in the trajectories of the dominant arm (mean ± SEM: 0.38 ± 0.02) as compared that of
443 the non-dominant arm (0.41 ± 0.02, P = 0.029, Fig. 8B). Differences in the average SD were
444 also significantly associated with the differences in average decorrelation between dominant
445 and non-dominant arms (Pearson's r = 0.648, P = 0.009, Fig. 8C). But we did not find
446 significant differences in the rate of decorrelation (β) between dominant (mean ± SEM: 0.145
447 ± 0.005) and non-dominant arms (0.151 ± 0.006, P = 0.19). Further, the *ZCR* (Fig. 8D) was

448 significantly higher in the dominant arm (mean ± SEM: 1.48 ± 0.03), compared to non-
449 dominant arm movements (1.40 ± 0.04, $P = 0.022$). Taken together these findings are consistent
450 with the notion that the higher skill associated with the dominant arm is associated with
451 signature of better trajectory control.
452
453 **Invariance in the extent of decorrelation across different speeds of movement**
454 We subjected the correlation analysis to different movement speeds, between fast and
455 slow conditions (Fig. 9A) to check how sensitive correlation analysis was to differences in
456 signal dependent noise that was expected to be greater for high movement speeds. The
457 maximum speed of fast movements (mean ± SEM: 37.03 ± 0.69 cm/s) was significantly higher
458 than the slow movements (mean ± SEM: 16.58 ± 0.39 cm/s, $P < 0.001$). Although, we found
459 that $\rho(t)$ for fast and slow movements were largely overlapping and that the $\bar{\rho}$ for fast
460 movements (mean ± SEM: 0.44 ± 0.03) was not significantly different from that of slow
461 movements (0.46 ± 0.05, $P = 0.377$, Fig. 9B) with a small effect size (Cohen's d – 0.29).
462
463 Overall, we used the time course of decorrelation between the initial and subsequent
464 time points as a measure of active online control, the rate of zero crossings around a mean
465 trajectory and the trend of z-scores as signatures of trajectory control, and compared these
466 measures in different contexts of goal and non-goal/return movements to show that 1) active
467 online control (or corrections) in trajectories was initiated as rapidly as 30 ms in goal-directed
468 finger movements and 16.67 ms in goal-directed whole-arm reach movements, providing
469 behavioral evidence for rapid internal feedback control during normative movements. 2) Such
470 rapid control also maintained the movements along a mean trajectory suggesting that the CNS
471 plans an average trajectory during goal-directed finger and whole-arm reach movements. 3)
472 Trajectory control was found to act at two distinct phases: at early (20 %) and late (around 90

%) phases along the time course of movement. 4) Online control was sensitive to the level of skill (across dominant and non-dominant) but was not sensitive to the range (across instructed fingers) or the speed (across fast and slow) of movements.

Discussion

Since Woodworth (1899), the detailed analysis of the kinematics of limb trajectories has provided insights to understand the relative contributions of motor planning from feedback control (Carlton, 1981; Abrams et al., 1990; Abrams and Pratt, 1993; Chua and Elliott, 1993). In addition to assessing the ability of the motor system to regulate variability throughout the trajectory (Khan et al., 2006), the coefficient of determination (R^2) has been used before as a within-trial estimate of the extent to which early kinematic markers (Carlton, 1981; Gordon and Ghez, 1987; Messier and Kalaska, 1999; Desmurget et al., 2005) such as peak acceleration and peak velocity determine end-point distributions. In this context, online control has been inferred by measuring the extent to which such markers do not predict the endpoint (i.e., lower R^2). Although inferential, such claims have been validated by manipulating factors such as the availability of visual feedback (Khan and Franks, 2003).

The correlation analysis used in this study uses a similar logic with some important differences that allowed us to reveal novel aspects of control during reaching movements. First, the earliest kinematic markers typically used are peak acceleration at ~150 ms is too late to reveal fast feedback control. Here, in contrast to previous works (Messier and Kalaska, 1999; Richardson et al., 2011; Kuang and Gail, 2015) that have emphasized the relationship of kinematic markers to the end of movement, we measured how quickly trajectories diverged from an initial starting posture. This analysis ensured that the starting variability between different task conditions such as goal and non-goal/return were the same and that any difference in control would be revealed at the earliest possible time. Further, the comparison with non-

goal movements was particularly useful, since it did not involve manipulation of target locations (Wolpert and Ghahramani, 2000; Gritsenko and Kalaska, 2010) or postures (Pruszynski et al., 2008, 2011) that would emphasize differences in sensory feedback control as opposed to internally driven control. Finally, and importantly, the absence of any difference in the extent of decorrelation for fast versus slow movements suggests that signal-dependent noise per se was not a factor contributing to the observed decorrelation signal (Fig. 9).

Trajectory control during goal-directed movements

In contrast to internal models of trajectory control, optimal feedforward/feedback control can also explain straight line trajectories and is supported by recent work showing the absence of corrective movements to a nominal trajectory in the presence of a perturbation (Cluff and Scott, 2015). Although, this result cannot be easily reconciled with our results, we suggest that a potential drawback of perturbation studies to assess trajectory control is the assumption that the original normative plan to be still relevant during corrections. In the context of target shift experiments, at least, this assumption is questionable as the original plan is expected to be modified or cancelled (Mirabella et al., 2008; Murthy et al., 2009). By extension, we assume a similar logic would also hold for external perturbations of the hand. Nevertheless, and interestingly, even in the study by Cluff and Scott (Cluff and Scott, 2015), when trajectory specifications such as timing and path were part of goal, corrections where directed to a normative trajectory. In this latter context, our experimental findings broadly agree with them (Cluff and Scott, 2015) as our goal directed finger and arm movements had timing constraints as compared to the non-goal movements.

Further, the demonstration of relatively fast task-related sensory feedback control (~50 ms) (Wolpert et al., 1998; Pruszynski et al., 2008) which could in principle shape trajectories during voluntary movement execution involving active participation of motor cortex

523 (Pruszynski et al., 2011) also is a key prediction of optimal feedback control models. However,
524 since movement in optimal feedback models (in the absence of trajectory costs) is driven by
525 costs associated with the current posture and the target position, they don't necessarily require
526 movements to crossover an average trajectory. This is in contrast with our observations of zero
527 crossings and that the trajectories starting farther away had a rapid propensity to converge
528 towards the average $z = 0$ line (Figs. 4 and 6). This suggests the presence of a mean planned
529 trajectory computed from the initial fixation to the target location in exocentric space.
530 Interestingly, this rapid convergence is prominent for goal movements as compared to non-
531 goal/return movements implying that they are not a consequence of a regression to the mean
532 effect (Fig 4B and 6B). Furthermore, we also observed greater zero crossings in the dominant
533 arm compared to the non-dominant arm, suggesting greater trajectory control in the former as
534 a reflection of greater skill (Fig. 8).

535 The other important aspect of control we tested is whether the CNS implements a fixed
536 extent of control or if it varies along different phases of movement. Modelling of perturbation
537 studies on arm movements has suggested that the extent of feedback controller gains are low
538 near movement initiation while they increase towards the end of movement as the hand reaches
539 the target (Liu and Todorov, 2007). We found that there were two distinct phases of control
540 (Fig 3D and 5D) which is reflected at time points where there is a relatively large change of
541 decorrelation in the early (trough at 20th percentile) and late (trough at 90th percentile) phases.
542 This pattern is reminiscent of via-point control (Bizzi et al., 1984) and further reinforces the
543 notion of a mean trajectory that can be efficiently corrected at two extreme postural positions
544 when the velocities of movements are relatively low and state estimation is more robust. Such
545 distinct troughs were not observed in a previous study since the initial variability was clamped
546 and no accuracy constraints were enforced towards the end of movement (Kuang and Gail,
547 2015). Implementing control close to the target location is obviously beneficial and has been

548 known since the time of Bernstein's seminal experiments (Bongaardt and Meijer, 2000), and
549 having a high degree of control earlier on has the obvious advantage of clamping variability to
550 manageable levels before the system is swamped by signal-dependent noise. Indeed, we
551 observed that the initial 10 % and 20 % of the response is predictive of the subsequent trajectory
552 variability (Fig. 7C). However, the relative absence of any decorrelation between the early and
553 late phases of control suggests that trajectory control is largely intermittent. Thus, we suggest
554 that optimal control models could incorporate such trajectory constraints in their cost function
555 (Mistry et al., 2013).

556

557 **Internal feedback control vs fast sensory feedback control**

558 Several studies have indicated signatures of relatively fast feedback control involving
559 reflexive arm movements that occur between 50 – 100 ms after the beginning of movements
560 (Messier and Kalaska, 1999; Pruszynski et al., 2008, 2011) during tasks that require posture
561 stabilization following mechanical perturbations. However, whether these feedback signals are
562 also at play during voluntary goal-directed movements is still not clear. Internal feedback
563 control implements corrections using an efference copy of the initiated motor command
564 (Kawato et al., 2003) to estimate the hand position via a forward model in the absence of delays
565 associated with sensory feedback (Desmurget and Grafton, 2000). However, to the best of our
566 knowledge, internal feedback has been shown to occur when goals and decisions are changed
567 during movements (Pisella et al., 2000; Gaveau et al., 2003; Desmurget et al., 2005; LoTemplio
568 et al., 2023) and help in fast error corrections in a feedforward manner. In the context of
569 normative movements such internal feedback control has been only studied in the context of
570 fast saccadic eye movements using a similar analysis (Richardson et al., 2011). Evidence of
571 internal feedback control has been shown in isometric force application (Gordon and Ghez,
572 1987) but it has not been demonstrated in normative voluntary reaching movements. In our

study, the initiation of control was indexed as the time point when significant differential decorrelations were observed between goal and non-goal movements, and this occurred as early as 30 ms in voluntary finger movements (Fig. 3C) and at 16.67 ms for voluntary whole-arm reach movements (Figs. 5C and 7D). We interpret this rapid control in reaching movements to be a signature of internal feedback control and not a consequence of feedforward postural correction as we would have expected a sharp decorrelation at the movement onset itself. This assertion is reflected in the decorrelation signal resembling a sigmoidal function rather than an exponential function. However, this early phase of decorrelation was followed with a later stage that is consistent with fast sensory feedback control with peaks at ~94 ms for goal finger and ~128 ms for goal movements of arm (Pruszynski et al., 2011).

Acknowledgements

We would like to thank all the subjects who participated in this study and colleagues in the labs of VSKM and AM for their assistance during the experiments. This research was supported by the Department of Biotechnology – Indian Institute of Science Partnership Program grant (DBT–IISc, *BT/PR27952/INF/22/212/2018*), Intramural funds from IISc (Institute of Eminence grant from the Ministry of Education), and Science and Engineering Research Board grant (SERB, *CRG/2022/000553*). NC was supported by the Prime Minister's Research Fellowship from the Ministry of Education (PMRF, *PM/MHRD-18-16074.03*).

Data Availability

Data for this research article is available on request from the corresponding author. The data is not available publicly due to privacy and ethical restrictions.

References

Abrams RA, Meyer DE, Kornblum S (1990) Eye-hand coordination: Oculomotor control in rapid aimed limb movements. Journal of Experimental Psychology: Human Perception and Performance 16:248–267.

Abrams RA, Pratt J (1993) Rapid Aimed Limb Movements: Differential Effects of Practice on Component Submovements. Journal of Motor Behavior 25:288–298.

Bizzi E, Accornero N, Chapple W, Hogan N (1984) Posture control and trajectory formation during arm movement. J Neurosci 4:2738–2744.

Bongaardt R, Meijer OG (2000) Bernstein's Theory of Movement Behavior: Historical Development and Contemporary Relevance. Journal of Motor Behavior 32:57–71.

Carlton LG (1981) Processing visual feedback information for movement control. Journal of Experimental Psychology: Human Perception and Performance 7:1019–1030.

Chakrabhavi N, Skm V (2019) Wrist Posture Does Not Influence Finger Interdependence. J Appl Biomech 35:410–417.

Chua R, Elliott D (1993) Visual regulation of manual aiming. Human Movement Science 12:365–401.

Churchland MM, Santhanam G, Shenoy KV (2006) Preparatory activity in premotor and motor cortex reflects the speed of the upcoming reach. J Neurophysiol 96:3130–3146.

Cluff T, Scott SH (2015) Apparent and Actual Trajectory Control Depend on the Behavioral Context in Upper Limb Motor Tasks. J Neurosci 35:12465–12476.

Desmurget M, Grafton S (2000) Forward modeling allows feedback control for fast reaching movements. Trends in Cognitive Sciences 4:423–431.

Desmurget M, Grafton S (2003) Feedback or feedforward control: End of a dichotomy. Taking action: Cognitive neuroscience perspective on intentional acts:289–338.

Desmurget M, Turner RS, Prablanc C, Russo GS, Alexander GE, Grafton ST (2005) Updating Target Location at the End of an Orienting Saccade Affects the Characteristics of Simple Point-to-Point Movements. Journal of Experimental Psychology: Human Perception and Performance 31:1510–1536.

Dick JPR, Benecke R, Rothwell JC, Day BL, Marsden CD (1986) Simple and complex movements in a patient with infarction of the right supplementary motor area. Movement Disorders 1:255–266.

Gaveau V, Martin O, Prablanc C, Pélisson D, Urquizar C, Desmurget M (2003) On-line modification of saccadic eye movements by retinal signals. NeuroReport 14:875.

Georgopoulos AP, Kalaska JF, Caminiti R, Massey JT (1982) On the relations between the direction of two-dimensional arm movements and cell discharge in primate motor cortex. J Neurosci 2:1527–1537.

Gordon J, Ghez C (1987) Trajectory control in targeted force impulses. III. Compensatory adjustments for initial errors. Exp Brain Res 67:253–269.

Gritsenko V, Kalaska JF (2010) Rapid online correction is selectively suppressed during movement with a visuomotor transformation. J Neurophysiol 104:3084–3104.

Harris CM, Wolpert DM (1998) Signal-dependent noise determines motor planning. Nature 394:780–784.

Hollander M, Wolfe DA, Chicken E (2013) Nonparametric Statistical Methods. John Wiley & Sons.

Kawato M (1999) Internal models for motor control and trajectory planning. Current Opinion in Neurobiology 9:718–727.

Kawato M, Kuroda T, Imamizu H, Nakano E, Miyauchi S, Yoshioka T (2003) Internal forward models in the cerebellum: fMRI study on grip force and load force coupling. In: Progress in Brain Research, pp 171–188 Neural Control of Space Coding and Action Production. Elsevier. Available at: http://www.sciencedirect.com/science/article/pii/S007961230342013X [Accessed January 6, 2020].

Keele SW (1968) Movement control in skilled motor performance. Psychological Bulletin 70:387–403.

Khan MA, Franks IM (2003) Online Versus Offline Processing of Visual Feedback in the Production of Component Submovements. Journal of Motor Behavior 35:285–295.

Khan MA, Franks IM, Elliott D, Lawrence GP, Chua R, Bernier P-M, Hansen S, Weeks DJ (2006) Inferring online and offline processing of visual feedback in target-directed movements from kinematic data. Neuroscience & Biobehavioral Reviews 30:1106–1121.

Kuang S, Gail A (2015) When adaptive control fails: Slow recovery of reduced rapid online control during reaching under reversed vision. Vision Research 110:155–165.

Li Z-M, Dun S, Harkness DA, Brininger TL (2004) Motion enslaving among multiple fingers of the human hand. Motor Control 8:1–15.

Liu D, Todorov E (2007) Evidence for the Flexible Sensorimotor Strategies Predicted by Optimal Feedback Control. J Neurosci 27:9354–9368.

LoTemplio SB, Lopes CL, McDonnell AS, Scott EE, Payne BR, Strayer DL (2023) Updating the relationship of the Ne/ERN to task-related behavior: A brief review and suggestions for future research. Frontiers in Human Neuroscience 17 Available at: https://www.frontiersin.org/articles/10.3389/fnhum.2023.1150244 [Accessed July 11, 2023].

Messier J, Kalaska JF (1999) Comparison of variability of initial kinematics and endpoints of reaching movements. Exp Brain Res 125:139–152.

Mirabella G, Pani P, Ferraina S (2008) Context influences on the preparation and execution of reaching movements. Cognitive Neuropsychology 25:996–1010.

Mistry M, Theodorou E, Schaal S, Kawato M (2013) Optimal control of reaching includes kinematic constraints. Journal of Neurophysiology 110:1–11.

Moran DW, Schwartz AB (1999) Motor cortical representation of speed and direction during reaching. J Neurophysiol 82:2676–2692.

Morasso P (1981) Spatial control of arm movements. Experimental Brain Research 42 Available at: http://link.springer.com/10.1007/BF00236911 [Accessed April 16, 2019].

Morris ME, Summers JJ, Matyas TA, Iansek R (1994) Current Status of the Motor Program. Physical Therapy 74:738–748.

Murthy A, Ray S, Shorter SM, Schall JD, Thompson KG (2009) Neural Control of Visual Search by Frontal Eye Field: Effects of Unexpected Target Displacement on Visual Selection and Saccade Preparation. Journal of Neurophysiology 101:2485–2506.

Oldfield RC (1971) The assessment and analysis of handedness: The Edinburgh inventory. Neuropsychologia 9:97–113.

Padoa-Schioppa C, Li C-SR, Bizzi E (2002) Neuronal Correlates of Kinematics-to-Dynamics Transformation in the Supplementary Motor Area. Neuron 36:751–765.

Pisella L, Gréa H, Tilikete C, Vighetto A, Desmurget M, Rode G, Boisson D, Rossetti Y (2000) An "automatic pilot" for the hand in human posterior parietal cortex: toward reinterpreting optic ataxia. Nat Neurosci 3:729–736.

Pruszynski JA, Kurtzer I, Nashed JY, Omrani M, Brouwer B, Scott SH (2011) Primary motor cortex underlies multi-joint integration for fast feedback control. Nature 478:387–390.

Pruszynski JA, Kurtzer I, Scott SH (2008) Rapid Motor Responses Are Appropriately Tuned to the Metrics of a Visuospatial Task. Journal of Neurophysiology 100:224–238.

Richardson BA, Ratneswaran A, Lyons J, Balasubramaniam R (2011) The time course of online trajectory corrections in memory-guided saccades. Exp Brain Res 212:457–469.

Rosenbaum DA (1985) Motor Programming: A Review and Scheduling Theory. In: Motor Behavior: Programming, Control, and Acquisition (Heuer H, Kleinbeck U, Schmidt K-H, eds), pp 1–33. Berlin, Heidelberg: Springer. Available at: https://doi.org/10.1007/978-3-642-69749-4_1 [Accessed June 17, 2023].

Scholz JP, Schöner G, Latash ML (2000) Identifying the control structure of multijoint coordination during pistol shooting. Experimental Brain Research 135:382–404.

Scott SH (2004) Optimal feedback control and the neural basis of volitional motor control. Nature Reviews Neuroscience 5:532–546.

Scott SH, Gribble PL, Graham KM, Cabel DW (2001) Dissociation between hand motion and population vectors from neural activity in motor cortex. Nature 413:161–165.

Summers JJ, Anson JG (2009) Current status of the motor program: Revisited. Human Movement Science 28:566–577.

Todorov E, Jordan MI (2002) Optimal feedback control as a theory of motor coordination. Nature Neuroscience 5:1226–1235.

Wolpert DM, Diedrichsen J, Flanagan JR (2011) Principles of sensorimotor learning. Nature Reviews Neuroscience 12:739–751.

Wolpert DM, Ghahramani Z (2000) Computational principles of movement neuroscience. Nature Neuroscience 3:1212–1217.

Wolpert DM, Ghahramani Z, Jordan MI (1995) An internal model for sensorimotor integration. Science (New York, NY) 269:1880–1882.

Wolpert DM, Kawato M (1998) Multiple paired forward and inverse models for motor control. Neural Networks 11:1317–1329.

Wolpert DM, Miall RC, Kawato M (1998) Internal models in the cerebellum. Trends in Cognitive Sciences 2:338–347.

Woodworth RS (1899) Accuracy of voluntary movement. The Psychological Review: Monograph Supplements 3:i–114.

Figures and Tables

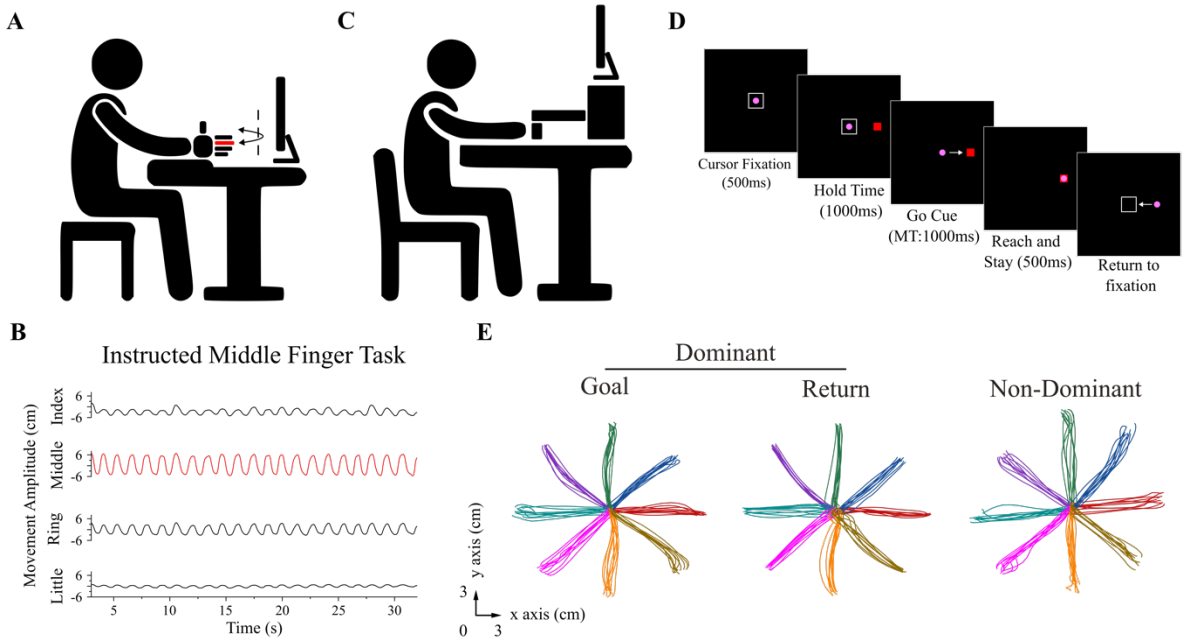

<u>Figure 1:</u> Task design of finger and arm experiments and their corresponding raw trajectories. *Finger experiment* (A and B) – A) The subjects rested their forearm and palm on a fixed platform in a neutral posture (pronation-supination), the thumb finger was restrained to the setup and the four fingers (index, middle, ring and little fingers) were suspended and free to move. On any given trial, the goal finger (middle finger, depicted with red color, in this case) was instructed to produce cyclic flexion (peaks) and extension (troughs) movements to specified landmarks shown on the stimulus screen (see methods). The phenomenon of finger enslavement led to involuntary movements in the other non-goal fingers (index, ring and little fingers). B) Sample traces of goal/instructed middle finger task. The traces were from the sensors attached to the distal phalanges of the fingers. In this figure, the goal-directed middle finger movement (red color trace) engaged non-goal movements in the index, ring, and little fingers. *Arm Experiment* (C, D and E) – C) The experimental setup consisted of a robotic arm that the subject held onto and performed simple reaching movements in the horizontal plane by looking at the stimulus presented on a screen placed in front. 3D motion trackers were mounted on the neck, shoulder, elbow, and wrist joints and on the dorsal side of the hand. The sensor on the hand was considered for the analysis in this study. D) The experimental protocol started with the subject fixating a pink circular cursor in a central fixation box for 500 ms. A red-colored target appeared at an eccentricity of 12cm on the screen. The target location was block randomized to appear at any of the 8 directions (0, 45, 90, 135, 180, 225, 270, and 315 degrees from the center). Subjects had to stay at the fixation for 1000 ms during hold time and the central fixation box disappeared marking the go cue to begin the movement. Subjects made simple smooth movements towards the target location within 1000ms and stayed there for an additional 500 ms to complete the trial. These movements were considered goal-directed movements. They then had to get back to the central fixation box for the start of the subsequent trial. These movements were considered as return movements and were not reward. The intertrial interval was 1500 ms. E) Sample traces of goal and return movements by the dominant arm and the goal movements by the non-dominant arm of one subject (10 trials each). The goal-directed movements were from the center to a target location while the return movements were from the target to the center.

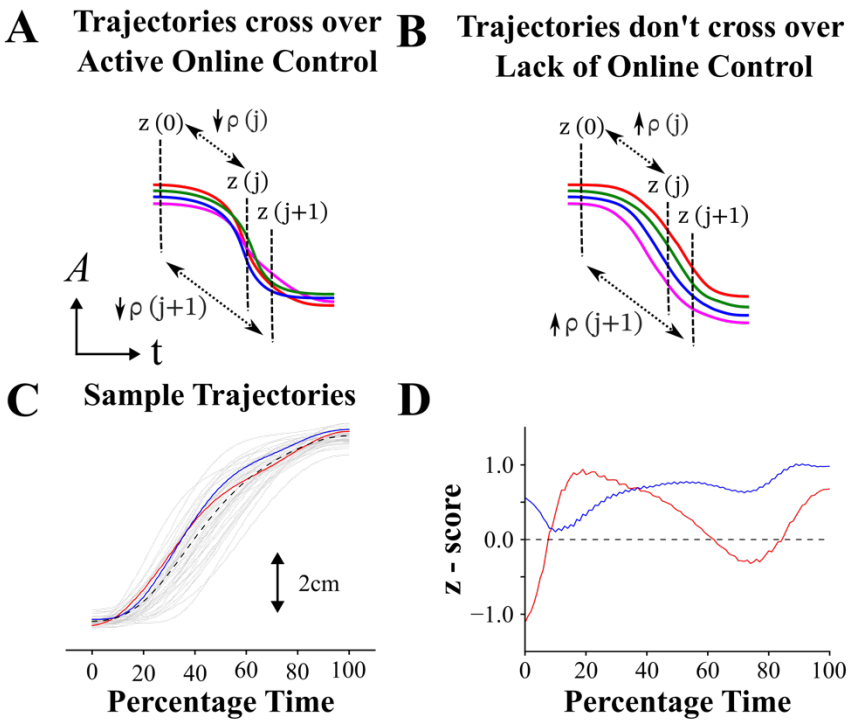

<u>Figure 2:</u> Behavioural signatures of online control and average trajectory planning. The colors red, blue, green, and pink in A and B represent individual trials of a given task. A) If the CNS implements active online control/correction based on it's initial posture, the *z*-scores at the start of the movement $z(0)$, is posited to change along the time course ($z(j)$ at any time $t = j$) resulting in crossovers among the trajectories. These crossovers could be captured by a decrease in the Spearman's correlation coefficient (ρ). By performing the correlation analysis between movement onset and the subsequent time instances $t = 0,\ldots,j,j+1,\ldots T$ (where T is the end of movement), we obtain a time varying $\rho(t)$. A low value of ρ indicates greater control. B) A case where the CNS does not implement online control i.e., the trajectories starting farther away from the average remain farther. The correlation coefficient ρ remains high and closer to 1 along the time course. C) Sample trajectories of the X coordinate of hand movements, directed along 0^0, of a single subject plotted against percentage time. The dashed black line represents the average trajectory and red and blue are two selected trials. D) Plot of *z*-scores for the red and blue trials/trajectories and the average trajectory, $z = 0$ (dashed black line), as depicted in C. To investigate if the implemented online control was directed towards an average planned trajectory, we computed the number of times the trajectories crossed the $z = 0$ line for a given set of trials (zero-crossing rate - *ZCR*, see methods). For example, the red trial has three zero-crossings during the movement and is considered to be under a stronger trajectory control, i.e., a greater propensity towards the average trajectory, while the blue trial had no zero crossings and is said to be under a weaker trajectory control.

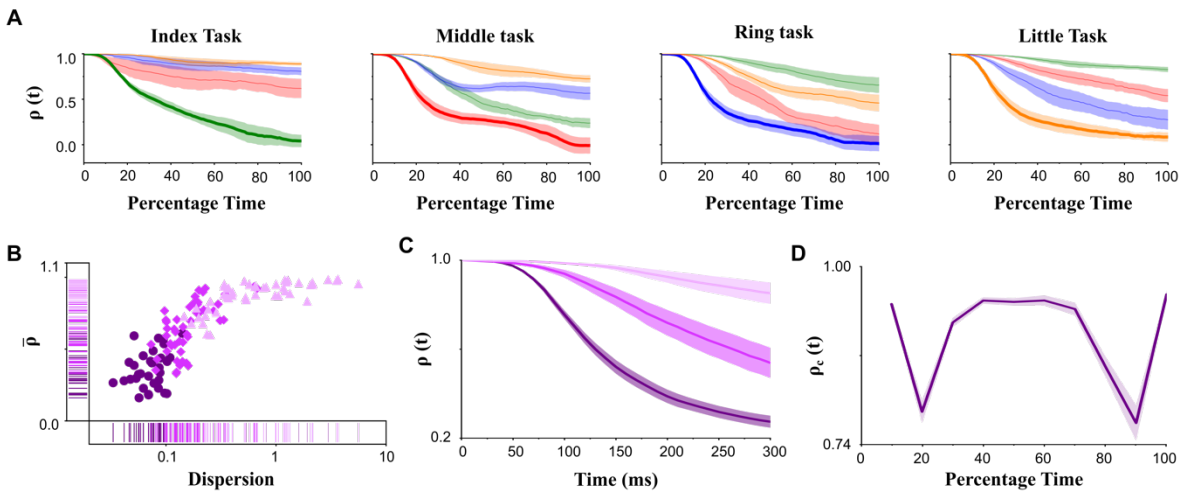

<u>Figure 3:</u> Spearman's correlation analysis of goal (bold) and non-goal finger movements. A) The trajectories of correlation co-efficient, $\rho(t)$, of the four fingers during goal directed index finger task, middle finger task, ring finger task, and the little finger task (mean ± SEM). The decrease in $\rho(t)$ was significantly higher in the goal finger in all the four tasks. Colors: green - index, red - middle, blue - ring, and orange - little fingers. B) Plot of average decorrelation ($\bar{\rho}$) vs trajectory dispersion showed that the goal fingers (circles) had the lowest $\bar{\rho}$ and lowest dispersion followed by that of non-goal neighboring fingers (diamonds) and non- neighboring (triangles) fingers. C) The trajectories, $\rho(t)$ (mean ± SEM), of goal finger, and non-goal neighboring and non-neighboring fingers plotted from movement onset to 300ms into the movement. The $\rho(t)$ in goal fingers significantly deviated from neighboring and non-neighboring fingers at 50ms and 30ms, respectively. D) Correlation analysis of goal finger between consecutive 10 % - time instances ($\rho_c(t)$, mean ± SEM). The two distinct phases of control, early control at 20 % and late control at 90 % of movement duration were observed. Colors in Fig. B to D: dark, medium, and light shades of purple represent goal, non-goal neighboring and non-goal non-neighboring fingers, respectively.

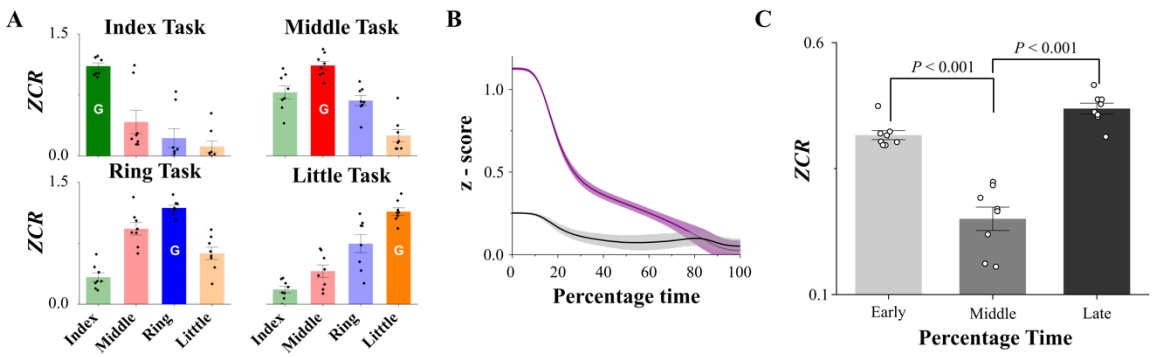

<u>Figure 4:</u> The zero-crossing rate (*ZCR*) of goal (bold) and non-goal finger movements and the average z-scores. A) *ZCR* computed from *z*-scores of goal and non-goal fingers (mean ± SEM) during goal directed index, middle, ring, and little finger tasks. *ZCR* was the highest in the goal finger of any task (further details in the Results, letter G on the bar represents the corresponding goal finger during any task). Colors: green - index, red - middle, blue - ring, and orange - little fingers. B) *z* - scores of goal fingers for trajectories (mean ± SEM) starting away ($|z| > 0.5$, purple) and closer ($|z| <= 0.5$, black) from the average initial posture ($z = 0$). The trajectories which started farther away from the average trajectory had a greater propensity to come towards the average trajectory, which is a potential signature of trajectory control. C) *ZCR* of goal fingers plotted for early (0 to 33 %, light grey), middle (34 to 66 %, medium grey) and late (67 to 100 %, dark grey) movement phases (mean ± SEM). We found that the *ZCR* was significantly greater in the early and late phases as compared to the middle phase (Adj. $P < 0.001$, both cases).

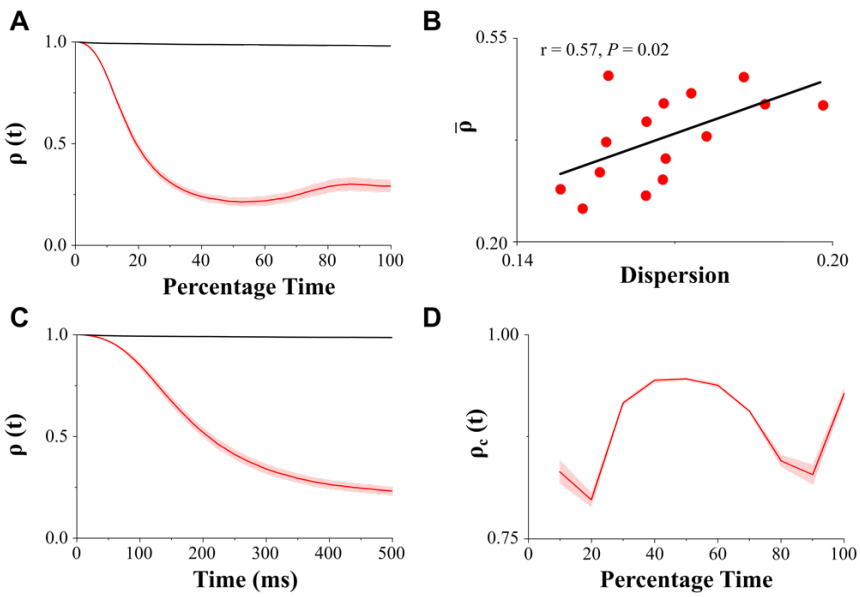

<u>Figure 5:</u> Spearman's correlation analysis of goal directed arm movements and during fixation. A) The correlation co-efficient, $\rho(t)$, plotted (mean ± SEM) for goal movements (red) was found to decrease along the movement duration while it stayed close to 1 during fixation condition (black). Goal movements were directed towards the target while the fixation was the time from movement onset to 1000 ms prior to the onset (in the negative direction of time) while the cursor was inside the fixation box. B) The average decorrelation ($\bar{\rho}$) was significantly associated with trajectory dispersion (Pearson's r = 0.57, P = 0.02). A lower correlation value corresponded with a lower trajectory dispersion. C) The correlation co-efficient, $\rho(t)$, plotted on actual time scale (mean ± SEM) for goal (red) and fixation (black) conditions. The time at which $\rho(t)$ of goal movements diverged from the fixation condition was found to be at 16.67 ms. D) Correlation analysis of goal movements between consecutive 10 % -time instances ($\rho_c(t)$, mean ± SEM). The two distinct phases of control i.e., early control at 20th percentile and late control at 80th and 90th percentile along the movement duration were observed.

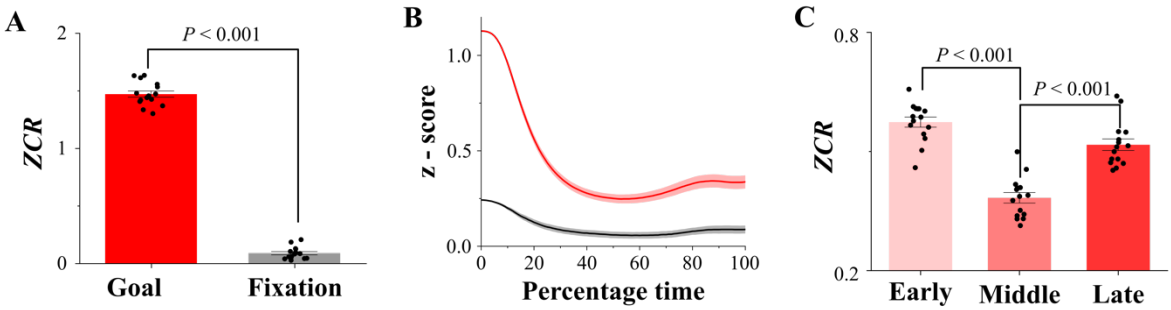

<u>Figure 6:</u> The zero-crossing rate (*ZCR*) of goal directed arm movements and during fixation and the average z-scores. A) *ZCR* (mean ± SEM) of goal directed movements (red) were significantly higher than during fixation (black, $P < 0.001$). B) The goal movements were segregated into ones starting farther away ($|z| > 0.5$, red) and closer ($|z| <= 0.5$, black) to the average trajectory ($z = 0$) and we found that the trajectories starting farther away had greater propensity towards the center than the closer ones (mean ± SEM). C) *ZCR* (mean ± SEM) of goal movements computed at the early (0 to 33 %, light red), middle (34 to 66 %, medium red) and late (67 to 100 %, dark red) movement phases. It was found that the *ZCR* was significantly greater during early and late phases as compared to the middle phase of movement (Adj. $P < 0.001$, both cases).

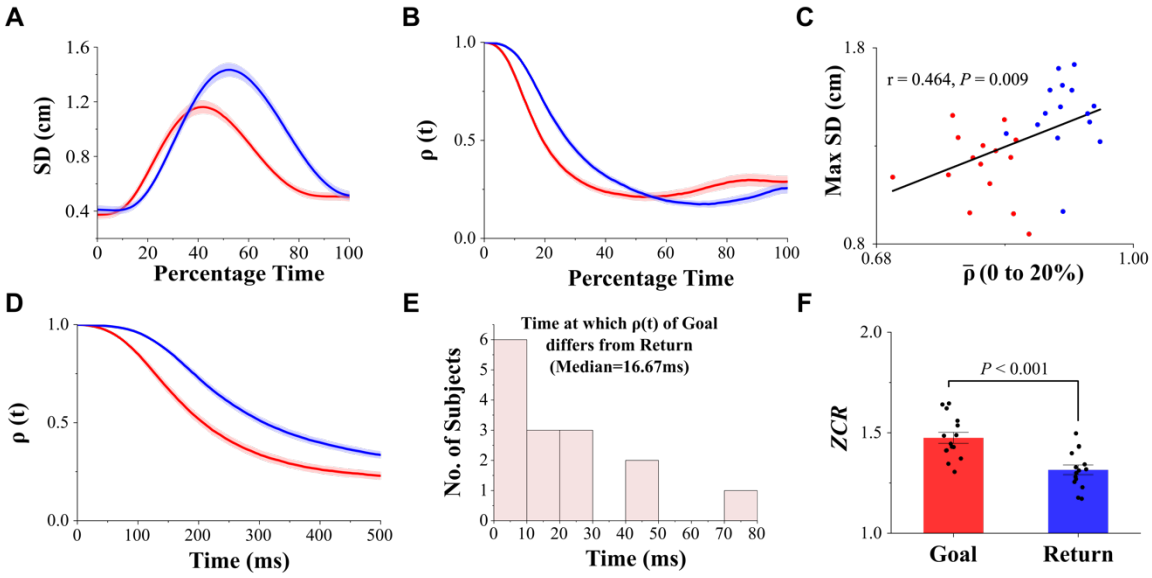

<u>Figure 7:</u> Differences in control between goal (red) vs return (blue) reach movements. A) The trajectory of inter-trial standard deviation (mean ± SEM) for goal and return movements. Return movements had greater SD than the goal movements. B) The trajectories of correlation co-efficient, $\rho(t)$, of goal and return movements (mean ± SEM). The average decrease in correlation ($\bar{\rho}$) was significantly higher in goal movements (P = 0.04). C) Correlation between $\bar{\rho}$, computed from 0 to 20 % time, with the maximum inter-trial standard deviation of goal and return trajectories. The initial decorrelation among trajectories was significantly associated with the maximum inter-trial variability (r = 0.464, P = 0.009) and that the goal movements had lower $\bar{\rho}$ and lesser variability than return movements. D) The variations in correlation co-efficient $\rho(t)$ on actual time scale from movement onset to 500ms into the movement (mean ± SEM), showed a steeper decrease for goal as compared to return movements. E) Histogram of the time at which the $\rho(t)$ of goal movements deviated from that of return movements. The deviation happened very early during the movement (median time =16.67ms). F) *ZCR* (mean ± SEM) of goal movements were significantly higher than that of return movements ($P < 0.001$).

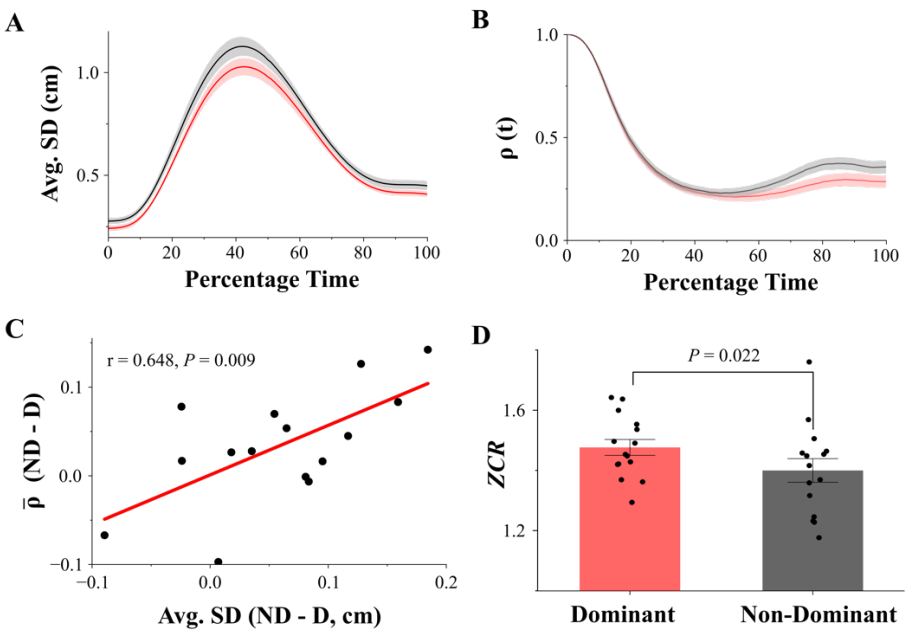

<u>Figure 8:</u> Differences in control between dominant (red) and non-dominant arms (black). A) Plot of inter-trial standard deviation (mean ± SEM) of trajectories of dominant and non-dominant arms. The non-dominant arm had a higher average SD than the dominant arm (P = 0.004). B) Correlation coefficient, $\rho(t)$ (mean ± SEM), of dominant and non-dominant arms. The average decorrelation was greater in dominant arm as compared to the non-dominant arm (P = 0.029). C) The differences in inter-trial SDs were significantly correlated with the differences the average decorrelation between dominant and non-dominant arms. ND – Non-Dominant, D – Dominant. D) The *ZCR* (mean ± SEM) in the dominant arm was significantly higher than the non-dominant arm (P = 0.022).

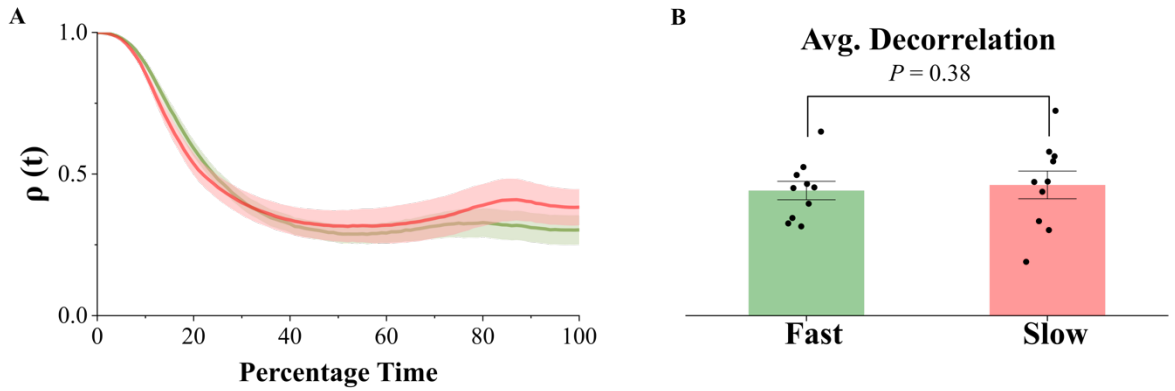

<u>Figure 9:</u> Correlation analysis on fast and slow reaching movements shows no difference in online control. C) Plot of correlation co-efficient trajectories, $\rho(t)$ (mean ±SEM), of fast (green) and slow (red) movements by the dominant arm. The $\rho(t)$ of fast and slow movements overlapped with each other. D) The average decorrelation ($\bar{\rho}$) was not significantly different between fast and slow movements (P = 0.38, Cohen's d = 0.29).

Goal Finger	$\bar{\rho}$	Non-Goal Finger	$\bar{\rho}$	Adj. *P*
Index	0.40 ± 0.05	Middle	0.76 ± 0.09	0.017
		Ring	0.89 ± 0.04	<0.001
		Little	0.93 ± 0.02	<0.001
Middle	0.36 ± 0.06	Index	0.56 ± 0.03	0.057
		Ring	0.72 ± 0.03	0.003
		Little	0.87 ± 0.03	<0.001
Ring	0.33 ± 0.05	Index	0.84 ± 0.04	<0.001
		Middle	0.51 ± 0.05	0.060
		Little	0.71 ± 0.04	<0.001
Little	0.35 ± 0.04	Index	0.92 ± 0.02	<0.001
		Middle	0.78 ± 0.04	<0.001
		Ring	0.59 ± 0.07	0.016

Table 1: Pairwise comparison of average decorrelation ($\bar{\rho}$) for goal and non-goal fingers (mean ± SEM). The *P* value in the last column is adjusted for multiple comparisons using Bonferroni correction. The $\bar{\rho}$ in goal finger was found to be significantly less than the non-goal fingers.

Goal Finger	Avg. Rate (β)	Non-Goal Finger	Avg. Rate (β)	Adj. P
Index	0.077 ± 0.012	Middle	0.043 ± 0.024	0.330
		Ring	0.030 ± 0.009	0.028
		Little	0.027 ± 0.006	0.012
Middle	0.115 ± 0.032	Index	0.060 ± 0.013	0.276
		Ring	0.057 ± 0.010	0.255
		Little	0.034 ± 0.006	0.060
Ring	0.118 ± 0.032	Index	0.029 ± 0.004	0.046
		Middle	0.078 ± 0.022	0.230
		Little	0.035 ± 0.005	0.045
Little	0.131 ± 0.031	Index	0.024 ± 0.006	0.005
		Middle	0.033 ± 0.006	0.025
		Ring	0.053 ± 0.016	0.020

Table 2: Pairwise comparison of rate of decrease in correlation (β) for goal and non-goal fingers (mean ± SEM). The *P* value in the last column is adjusted for multiple comparisons using Bonferroni correction. The average rate of decrease in $\rho(t)$ in goal finger was found to be significantly higher than the non-goal non-neighboring fingers but was not different from the neighboring fingers.

Goal Finger	Zero Crossing Rate	Non-Goal Finger	Zero Crossing Rate	Adj. P
Index	1.11 ± 0.04	Middle	0.42 ± 0.14	0.003
		Ring	0.22 ± 0.12	<0.001
		Little	0.12 ± 0.07	<0.001
Middle	1.11 ± 0.05	Index	0.78 ± 0.08	0.036
		Ring	0.68 ± 0.06	0.003
		Little	0.25 ± 0.08	<0.001
Ring	1.18 ± 0.03	Index	0.33 ± 0.05	<0.001
		Middle	0.93 ± 0.08	0.045
		Little	0.63 ± 0.08	<0.001
Little	1.14 ± 0.05	Index	0.18 ± 0.04	<0.001
		Middle	0.41 ± 0.08	<0.001
		Ring	0.75 ± 0.11	0.015

Table 3: Pairwise comparison of zero crossing rate (*ZCR*) of goal and non-goal fingers (mean ± SEM). The *P* value in the last column is adjusted for multiple comparisons using Bonferroni correction. The *ZCR* in goal finger was found to be significantly higher than the non-goal fingers.